

Zinc-Rich Paint As Anode for Cathodic Protection of Steel in Concrete

Das, S.C. , Pouya, H.S. and Ganjian, E.

Post-print deposited in [Curve](#) November 2015

Original citation:

Das, S.C. , Pouya, H.S. and Ganjian, E. (2015) Zinc-Rich Paint As Anode for Cathodic Protection of Steel in Concrete . Journal of Materials in Civil Engineering, volume 27 (11): Article number 04015013. DOI: 10.1061/(ASCE)MT.1943-5533.0001243

[http://dx.doi.org/10.1061/\(ASCE\)MT.1943-5533.0001243](http://dx.doi.org/10.1061/(ASCE)MT.1943-5533.0001243)

American Society of Civil Engineers

Copyright © and Moral Rights are retained by the author(s) and/ or other copyright owners. A copy can be downloaded for personal non-commercial research or study, without prior permission or charge. This item cannot be reproduced or quoted extensively from without first obtaining permission in writing from the copyright holder(s). The content must not be changed in any way or sold commercially in any format or medium without the formal permission of the copyright holders.

CURVE is the Institutional Repository for Coventry University

<http://curve.coventry.ac.uk/open>

Zinc-Rich Paint as Anode for Cathodic Protection of Steel in Concrete

Sunil C. Das¹; Homayoon Sadeghi Pouya²; and Eshmaiel Ganjian³

Abstract: This paper describes the findings of the experimental works undertaken to investigate the performance of zinc-rich paint (ZRP) to provide cathodic protection to chloride-contaminated RC structures. The program of experimental works was designed and conducted to assess four principal properties, viz (1) conductivity, (2) adhesion with concrete (short term and long term), (3) durability, and (4) electrochemical polarization. These properties considered together define the ability and effectiveness of the materials to act as an anode for impressed current cathodic protection. The research findings indicated that a specific proprietary ZRP product showed that optimum conductance was obtained with three coats producing a 280–320 μm thickness, with good adhesion to the concrete substrate, in which values obtained ranged between 1.65 and 3.5 MPa with and without applied current. It was capable of withstanding/supporting high levels of current, i.e., more than 300 mA/m², and the service life of the ZRP coating was estimated to be well in excess of 20 years at an applied current density of 10 mA/m². DOI: 10.1061/(ASCE)MT.1943-5533.0001243. © 2015 American Society of Civil Engineers.

Author keywords: Zinc-rich paint anode; Cathodic protection; Corrosion; Chloride; Reinforcement.

Introduction

In recent years, there has been considerable interest and a substantial increase in the use of zinc and zinc alloy anodes and also some limited use of aluminum/aluminum alloy anodes for the cathodic protection (CP) of steel RC structures (Covino et al. 2002; Bullard et al. 2009). Zinc anodes in various forms have been developed over the years [SHRP-S-337 1993 (Strategic Highways Research Program 1993); National Cooperative Highway Research Program (NCHRP) Report 398 2009 (NCHRP 2009)], and a number of them are now commercially available. However, the performances of zinc anodes to provide sacrificial cathodic protection to steel reinforcement in chloride-contaminated concrete are found to be less than adequate to provide full protection to atmospherically exposed RC structures in the long term (Covino et al. 2002). Sagüés and Powers (1996) reported that the absence of direct wetting of the anode surface could result in long-term loss of adequate current delivery, even when the concrete was in contact with air of 85% relative humidity (RH) when sprayed zinc on the surface of concrete was used as sacrificial anodes. Therefore, the application of zinc has traditionally been limited mainly to mitigate the incipient anode effect, but researchers and corrosion scientists in the United States, particularly the Department of Transportation (DOT) of Oregon, have actively encouraged applying thermally sprayed (TS) zinc and also Zn-Al or Al alloy coatings on a concrete surface,

which is called metalizing the concrete (Apostolos 1984). Since a trial installation in 1984 (Apostolos 1984), more than 80,000 m² TS zinc CP systems, both sacrificial or impressed current CP, have been installed in Oregon alone over the period between 1995 and 2005 (Covino et al. 2002; Bullard et al. 2009).

There is ample literature on the theoretical basis of the subject and the applications of TS zinc anodes in various forms (Kepler et al. 2000). For the CP of RC structures, some pioneered publications can be found (Covino et al. 2002; Bullard et al. 2009; NCHRP Report 398 2009).

Zinc-Rich Paints: Application and Chemical Composition

Zinc-rich paints (ZRPs) are widely used as an anticorrosion paint on ferrous substrates, an alternative to hot-dip galvanizing (HDG), an under coat or top coat, and also as a touch-up coat on galvanized steel to provide corrosion protection of steel in moderately severe environments and cathodic protection to steel substrates in corrosive marine atmospheric environments (Morcillo et al. 1990; Abreau et al. 1996; Hare 1998). It is often quoted as cold galvanizing. It has also been effectively used to protect steel structures fully and/or partially immersed in sea water, e.g., the ship's hull, offshore platforms, and jetties (Zhang 1996).

The metallic zinc content in the dry film is a very important parameter to be emphasized in the technical specifications of zinc-rich paints. However, as observed by Lindquist et al. (1985), this parameter is not the only factor determining the performance of this kind of paint. For example, Fragata et al. (1987), Amo and Giudice (1990), and Pereira et al. (1990) verified that the chemical nature of the binder and zinc particle size are also very important.

The zinc dust, which has a spherical or lamellar shape or a combination of both, is dispersed in an inorganic, usually orthosilicates, or organic binder, usually epoxies (Wicks et al. 1994). These particles must be in electrical contact between themselves and the metallic substrate to ensure a well-established electrical conduction within the coating. In such conditions of percolation, a galvanic coupling is created between zinc and the substrate (steel), which is nobler than the zinc. Then, zinc can preferentially dissolve, acting

¹Principal Engineer, Amey, International Design Hub, 20 Colmore Circus, Birmingham B4 6AT, U.K.

²Research Fellow, Faculty of Engineering and Computing, Dept. of Civil Engineering, Architecture and Building, Coventry Univ., Sir John Laing Building, Coventry CV1 5FB, U.K.

³Reader in Civil Engineering Materials, Faculty of Engineering and Computing, Dept. of Civil Engineering, Architecture and Building, Coventry Univ., Sir John Laing Building, Coventry, CV1 5FB U.K. (corresponding author). E-mail: E.Ganjian@coventry.ac.uk

Note. This manuscript was submitted on March 31, 2014; approved on November 12, 2014. **No Epub Date**. Discussion period open until 0, 0; separate discussions must be submitted for individual papers. This paper is part of the *Journal of Materials in Civil Engineering*, © ASCE, ISSN 0899-1561/9/\$25.00.

76 as a sacrificial pigment and allowing a cathodic protection of
77 the substrate. Many studies (Fleu et al. 1989; Pereira et al. 1990,
78 Armas et al. 1992) exist in the literature and relate the protection
79 mechanisms and degradation processes of such coatings. Physico-
80 chemical properties and corrosion resistance of solvent-based ZRPs
81 strongly depend on pigment, i.e., zinc, volume concentration
82 (PVC), shape, and size of the zinc dust (Vilche et al. 2002; Abreu
83 et al. 1997). In common liquid ZRP, zinc is usually introduced as
84 spherical pigments, with a mean diameter ranging from 5 to 10 μm .
85 To ensure good electrical contacts between zinc pigments and
86 the steel substrate, a high pigment concentration is required, which
87 is usually above 60% by volume in solvent-based ZRPs (Vilche
88 et al. 2002).

89 A literature search indicated no prior works on ZRP as an anode,
90 particularly as an impressed current CP anode for the CP of RC,
91 except for some trials as a sacrificial anode (Apostolos 1984), but
92 the main aim of these trials was to compare and contrast the per-
93 formance of ZRP applied directly on exposed steel reinforcement
94 to that of the galvanized steel reinforcement and/or other anticor-
95 rosion paints for the exposed and corroding reinforcement. A case
96 study (Das 2012) described the application of a ZRP on partially
97 immersed concrete piles at Bangor Harbour to provide sacrificial
98 cathodic protection (Das 2012). The specific objectives of this re-
99 search were to evaluate the performance of zinc-rich paints as an
100 impressed current anode system for cathodic protection (ICCP) of
101 RC structures.

102 Experimental Program

103 A review of commercially available zinc-rich paints has identified
104 one proprietary product consisting of 96% zinc as the most prom-
105 ising candidate material for this research. This off-the-shelf com-
106 mercially available ZRP product is a single-pack zinc coating that
107 is easy to apply by brush, roller, spraying, or dipping under any
108 atmospheric condition. Because of commercial confidentiality, it
109 is not possible to disclose the name of the manufacturer or the full
110 chemical composition of the ZRP. The main components are zinc
111 powder, aromatic hydrocarbons, and a binder. A dry layer of paint
112 consists of 96% zinc, which is pure to 99.995% and homo-
113 geneously dispersed throughout the layer. The ZRP coating dries
114 by evaporation of the solvent. Further, the unique characteristic
115 of this ZRP is that each new layer reliquidizes the former zinc layer so
116 that both layers form one homogeneous layer (Das 2012).

117 Four sets of experiments were designed and conducted in this
118 part, including (1) a conductivity test, (2) adhesion test, (3) durabil-
119 ity test, and (4) polarization test. For each set of tests, special con-
120 crete test specimens were made with slight variations in the
121 concrete mix design but basically keeping similar characteristic
122 concrete properties. The concrete mix designs were to create two
123 different types of concrete, with a low and high water-to-cement
124 (w/c) ratio of 0.53 and 0.83, respectively. Some concrete specimens
125 with different levels of chloride deliberately added in the concrete
126 mix to stimulate active corrosion of steel reinforcement were also
127 produced.

128 Specimen Preparations and Test Setup

129 The specimens' preparation and procedures for each test program
130 are briefly described subsequently.

131 Conductivity Test

132 Conductance of the ZRP material was determined by measuring
133 the cross-film resistance. This was undertaken to determine an

optimum number of coats applied on a nonconducting substrate
to achieve an optimum conductivity.

134
135
136 A total of three 180 \times 250-mm compressed hardboard (wood
137 pulp) specimens with electrical connections comprising of two thin
138 copper strips (1.5 \times 10 mm \times 180 mm) with electrical wires sol-
139 dered were fixed onto the hardboard using an epoxy adhesive be-
140 fore ZRP coating. All hardboard specimens were given a total of
141 five coats, with the exception of Hardboard Number 3 (HB 3),
142 which was given a total of 10 coats. Each measured coat was aimed
143 at achieving a wet film mass of 12.4 g, which corresponds to a
144 theoretical dry film thickness of 60 μm . For all hardboard speci-
145 mens, when each applied coat has become sufficiently dry (approx-
146 imately 24 h), the resulting thickness of paint was measured
147 by using a digital vernier calliper (0–150 mm range; accuracy of
148 0.01 mm). Measurements were carried out at approximately 20
149 places to calculate an average thickness.

150 The direct current (DC) resistance of the coating (dry) of each
151 application was measured across the two copper strips using a stan-
152 dard digital volt meter (DVM). A number of measurements were
153 made for each coat over a period of at least 24 h or until a constant
154 reading was obtained. This was repeated following each coat
155 application.

Adhesion Strength

156
157 The adhesion strength was determined using the adhesion tester
158 Elcometer 106/6, all in accordance with the procedure recom-
159 mended by CIRIA (1993) and Elcometer (2004). A total of two
160 grades of concrete specimens, representing low w/c ratio and high
161 w/c ratio concrete, with target compressive strengths of 40 and
162 20 MPa, respectively, were cast in accordance with BS EN 206-1
163 (British Standards Institution 2000).

164 Table 1 gives the concrete mix design. For each concrete mix,
165 three (three No.) cube samples (150 \times 150 \times 150 mm) with no
166 chloride added to the test specimen were produced. A total of 2 days
167 after demolding, specimens were fully immersed in a curing tank
168 for 28 days and then allowed to dry in air before zinc coating.

169 To assess the effect of the concrete surface profile on the adhe-
170 sion strength of the ZRP coating, each grade of concrete specimens
171 was prepared to produce three different levels of surface roughness.
172 These are defined as (1) very high roughness (VHR), where most of
173 the aggregates were exposed; (2) high roughness (HR), where some
174 aggregates were exposed; and (3) medium roughness (MR), where
175 mainly the cement laitance layer was removed with little or no
176 aggregates exposed. Table 2 summarizes the tools used to create
177 surface profiles and the roughness classifications that are qualita-
178 tive on the basis of visual assessment.

179 The prepared concrete substrates were then coated with the ZRP.
180 A total of four coats were applied by brush to achieve a dry film
181 thickness (DFT) of approximately 200–350 μm . The coating of
182 ZRP by brush was found to be as simple as painting with domestic
183 emulsion paint. Each coat of paint was applied after allowing the
184 previous coat to dry for 24 h. After each application of paint, the
185 wet and dry mass of paint was measured, and finally the total mass
186 of dry paint of a number of coats was measured to determine the
187 total DFT. The adhesion strength of the ZRP was determined first
188 within 24 h after the final coat was allowed to dry and also after
189 allowing the dry paint film to age for a total 56 days, i.e., at the end
190 of the environmental durability testing described under Item 3.
191 The adhesion strength was determined using an adhesion tester
192 Elcometer 106/6, all in accordance with the procedure recom-
193 mended by CIRIA (1993) and Elcometer (2004). Briefly, the test
194 was conducted using 20-mm-diameter high-strength aluminum al-
195 loy dollies bonded onto the test surface by means of an epoxy resin

Table 1. Concrete Mix Proportions for Environmental Cube Specimens

Component	Concrete mix design	
	Low w/c G	High w/c P
Water-cement ratio	0.50	0.80
Ordinary Portland cement (kg/m ³)	300	200
Water (kg/m ³)	150	160
Uncrushed coarse aggregate (kg/m ³) (4.75–10 mm size)	1,300	1,175
Fine aggregate (kg/m ³) (sand) \approx 65% passing 600- μ m sieve	670	867
Slump test (mm)	\approx 10	\approx 20
Amount of compaction (vibrating table) (m/s ²)		
Shock table mode of vibration (\approx 8 g)	Cubes: G1–G5	Cubes: P1–P5
Curing process (2 days after demolding specimens)	Fully immersed in curing tank for 28 days and then allowed to dry in air before zinc coating	

Table 2. Summary Illustrating the Methodology and Engineering Judgment Used to Obtain Different Levels of Concrete Substrate Roughness through Trial Experimentation

Substrate roughness degree (terminology)	Tool utilized	Manual/automatic	Degree of aggregates exposed
VHR	Needle gun (compressed air)	Automatic	Most aggregates exposed
HR	Needle gun (compressed air)	Automatic	Some aggregates exposed
MR	Wire brush	Manual	Little/no aggregates exposed

adhesive. After curing of the resin, the adhesion tester was placed in position and the indicator dial was set to zero. Then, the hand wheel was tightened until the pulling force to the dolly caused the break away from the surface and the pull-off force was read off the instrument dial, and the results were converted to bond strength in MPa.

Environmental Durability

The objectives of the environmental durability test were to investigate the effect of humidity and temperature on zinc paint with and without CP and to assess, at the end of 40 cycles, the bond strength between paint and concrete. A total of three cubes were used for this experiment. A total of three 150-mm concrete cubes were prepared with the concrete mix design, as given in Table 1, and cast with 0, 1, and 3% chloride by the mass of cement (as NaCl) added to the concrete mixes. The cube samples were cast with two 10-mm-diameter steel reinforcement bars, one macrocell corrosion-measuring probe named beta-probe without NaCl, and one Ag/AgCl reference electrode, as shown in Fig. 1. Cable connections to elements were insulated with heat-shrink sleeves. Specimens were cured for 7 days in the curing tank at 20°C and 98% RH each. The cubes were then applied with three coats of zinc paint on the top face, allowing 24 h between coats for each coat to dry. The zinc coating thickness for each cube was determined. The thickness of the ZRP applied on the concrete surface of all the cubes was calculated and found in the range of 232–234 μ m.

The cubes were then placed in plastic trays. The painted top surface was faced up and partially filled with test solutions without covering the top zinc coated surface: one tray with distilled water, one tray with a 1% chloride solution, and one tray with a 3.5% chloride solution. All three cubes were then placed in the environmental chamber exposed to 40 temperature and humidity cycles, and each cycle was set for 24 h. The chamber started at 20°C and 50% humidity. Then, it ramps to 50°C and 90% humidity in 1 h and remains in these conditions for another 8 h. Then, it ramps down to 20°C and 50% humidity in 1 h and remains in these environmental conditions for another 14 h.

The procedures used for the environmental durability test are briefly described subsequently. Before environmental testing commenced, the three specimens were placed in their respective trays, and the potentials of the rebars were monitored, with respect to Ag/AgCl reference electrodes, once a day for 14 days. The corrosion current of the rebars was also measured by connecting a precision resistor across the rebars and the beta-probes (macrocorrosion cell). The environmental chamber was set at 50°C, 90% RH, and then the minicathodic protection system was set up by connecting the cables from the rebars to the negative terminal and the cable connected to the copper strip (as a primary anode) embedded in the ZRP anode system to the positive terminal of a constant current/constant voltage DC power supply unit. Fig. 2 gives the electrical circuit diagram for the test. Then, the power supplies to the environmental chamber and CP system were switched on to begin testing, and at the end of each cycle, a number of parameters were measured

**Fig. 1.** Arrangement of rebars, reference electrode, and probe for environmental durability test

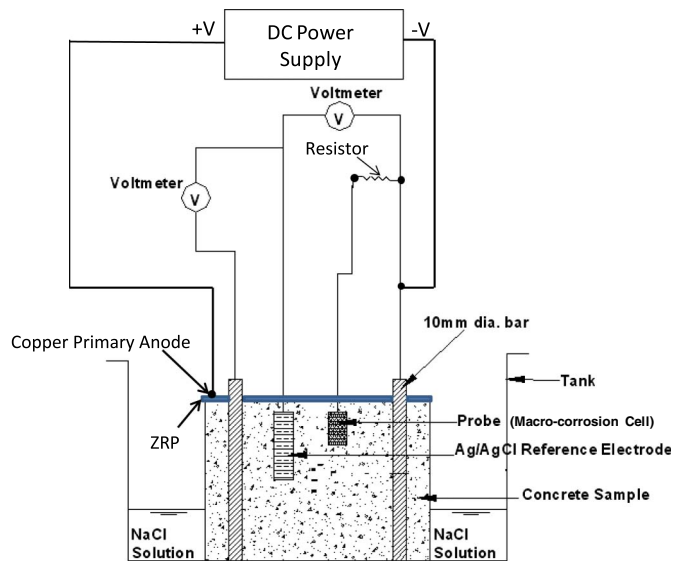


Fig. 2. Electrical circuit diagram for durability (cube) test



Fig. 3. Beams and circuit setup of cathodic polarization experiment

F2:1

F3:1

at 1 h, 24 h, and then once a day for 40 cycles. These were (1) cell voltage and cell current, (2) cathode (rebars) potential, (3) corrosion current with the beta-probe, and (4) zinc paint and concrete surface, which were visually examined after applying a current. The operating voltage throughout the testing varied between 1.5 and 2.1 V. Finally, at the end of 40 cycles, the bond strength between the paint and concrete was determined.

255 **Electrochemical Performance: Polarization Beam Test**

The principal philosophy behind these experiments is to set up minicathodic protection systems utilizing the zinc coating and assess the following performance parameters:

1. Current throwability, i.e., the coating's ability to uniformly distribute an impressed current to the corroding embedded rebar from primary anodes;
2. Polarization characteristics of coating; and
3. Cathodic polarization of the rebar by the coating.

For this test, concrete beam specimens (Fig. 3), which were 200 × 150 × 750 mm long with two 10-mm-diameter steel bars at 90-mm spacing and 50-mm cover, were cast. Table 3 gives the concrete mix design parameters for these beams, with 2 and 4% chloride by mass of cement deliberately added in the mix to ensure that the embedded bars were in a corrosively active state. To monitor the performance of the coatings and steel bars, three miniaturized mixed metal oxide/titanium (MMO/Ti) reference electrodes were embedded into the beams, except for the beam with no chloride (Beam A), where one additional Ag/AgCl reference cell (Reference Cell #1) was installed for calibration. The potential values obtained with respect to the MMO/Ti reference electrodes were converted to values with respect to the Ag/AgCl reference cells. A total of three beam specimens were prepared by wire brushing the top surface before applying the zinc coating.

The dust on the surface was cleaned with noncontaminated compressed air. A copper strip (primary electrode) was installed 1 cm away from one edge of the top of the beam. The top face of each beam specimen was painted with three layers of ZRP, making sure that the copper strip is covered with the zinc paint. Table 4 gives the total dry coat thickness (DFT) on each specimen. The base and sides of the beams were sealed with epoxy pitch paint (Epilux 5) to minimize loss of moisture during the experiments.

Table 3. Concrete Mix Design Parameters for Electrochemical Performance Test (Polarization Beam)

Mix	Cement (kg)	Sand (kg)	Gravel (kg)	Water (kg)	Chloride (kg)
Control	6.08	12.89	16.54	3.14	0
2% chloride	6.08	12.89	16.54	3.14	0.1216
4% chloride	6.08	12.89	16.54	3.14	0.2432

T3:1

T3:2

T3:3

T3:4

Table 4. Dry Film Thickness on Beam Test Specimen

Beam	Dry coat			Total thickness (μm)
	First coat thickness (μm)	Second coat thickness (μm)	Third coat thickness (μm)	
1 (Control)	114	95	73	282
2 (2% chloride contaminated)	110	71	73	254
3 (4% chloride contaminated)	104	81	68	253

T4:2

T4:1

T4:3

T4:4

T4:5

The specimens were placed in a tank containing water so that the samples were partially submerged. The beams were also sprayed regularly with water every 2 days to keep them moist. The environmental temperature condition was constant at 20 ± 1°C. This part of the experiment was carried out in accordance with BS EN 12696:2000 "Cathodic Protection of Steel in Concrete" (BS EN 12696 2012).

The cathodic polarization characteristics of the coating were assessed at three levels of current, i.e., 10, 20, and 30 mA, which were approximately 110, 220, and 333 mA/m² of the ZRP coating/concrete area. The beam specimens were connected in a series circuit to the power supply. Fig. 4 gives the electrical circuit diagram for this test.

The current was supplied for 7 days for each current level, and the polarization characteristics were monitored every day. After 7 days, the current was switched off (instant off potentials were recorded) for 24 h. The depolarization was monitored over several time intervals in accordance with BS EN ISO 12696 (2012) throughout the day to obtain decay potential curves and thus relates to the characteristic cathodic protection of the steel reinforcement.

287

288

289

290

291

292

293

294

295

296

297

298

299

300

301

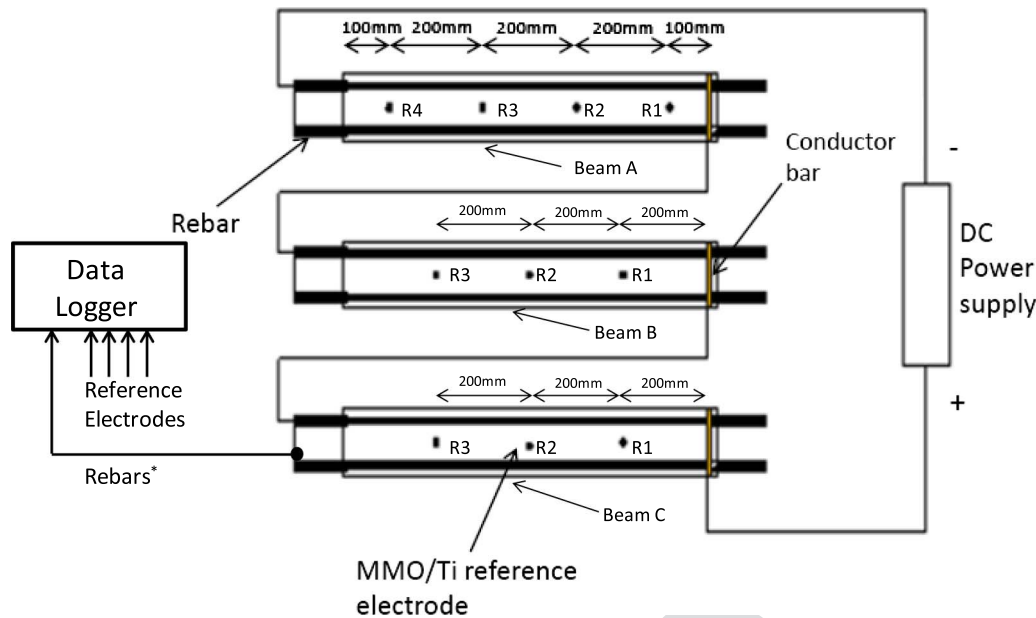
302

303

304

305

306



*Individual cables from rebars and reference electrodes are terminated to a data logger

Fig. 4. Electrical circuit diagram for polarization (beam) test

F4:1

307 Experimental Results and Discussion

308 The results of the experimental works investigating the conductance, adhesion, environmental durability, and electrochemical characteristics of ZRP to perform as an anode for the impressed current cathodic protection system to mitigate the corrosion of reinforcements in chloride-contaminated concrete are summarized and discussed subsequently.

314 Conductance (Cross-Film Resistance)

315 The cross-film resistances were measured after each coating application using a digital multimeter until the resistance showed little change in values with further coating application. Data for the cross-film resistance against the number of coats applied were statistically analyzed using the R^2 factor to assess the trend. The results in Table 5 and Fig. 5 show that the cross-film resistance decreasing exponentially, and the optimum minimum resistance was obtained with three or four coats, i.e., with a coating thickness of between 286 and 322 μm of DFT. A further number of coats, e.g., up to five coats plotted in Fig. 5, showed an insignificant reduction in cross-film resistance.

326 Adhesion Strength

327 The initial test program identified that the ZRP coating used had good adhesion properties to the concrete substrate. The average values ranges between 3.11 and 1.78 MPa for the concrete mix with a low water-cement ratio ($w/c = 0.50$) and for the concrete mix with a high water-cement ratio ($w/c = 0.80$), respectively. These tests were carried out within 48 h following drying of the final coat. The tests results obtained after allowing the paint to age for 56 days in total, i.e., 2 days for paint coats to dry plus 14 days of initial testing plus 40 days in the environmental chamber, for both low and high w/c concrete showed some increase in bond strength for both the low w/c concrete (average value was 3.35 MPa) and high w/c concrete (average value was 2.53 MPa) (Table 6). Detailed study on the failure mode(s) of ZRP applied on the concrete surface

was outside the scope of the present investigations; however, the adhesive strength values quoted in this evaluation are the values with a failure criterion in which the area of fracture is greater than 15% with respect to failure between the substrate and coating. The results to assess the effect of three different levels of surface roughness on the adhesion strength of ZRP coating indicated that HR, in which some aggregates were exposed, to MR, in which mainly the

340
341
342
343
344
345
346

Table 5. Summary Table of Cross-Film Resistance Measurement

Parameter	HB 1(a)	HB 1(b)	HB 2	HB 3
DFT by measurement (μm)	286	296	322	301
Optimum low resistance ($\text{k}\Omega$)	142	124	44	61
Environmental condition	Outdoor	Indoor/outdoor	TCP	
Drying time (h)	2-3	Variable	24	

T5:1
T5:2
T5:3
T5:4
T5:5

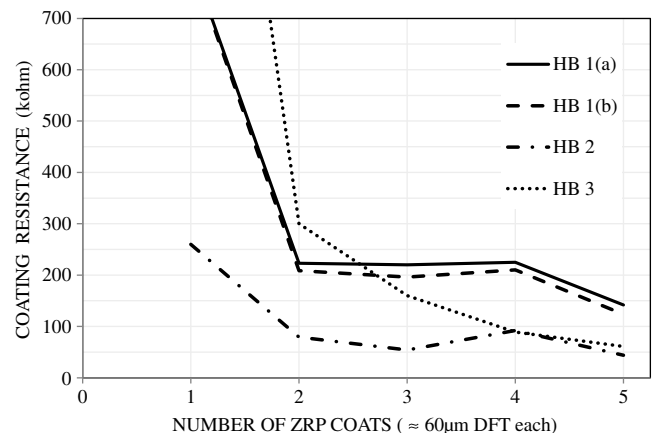


Fig. 5. Coating resistance versus number of coats

F5:1

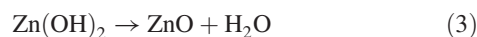
Table 6. Bond Strength Results With and Without CP under Environmental Conditions and Comparison with Other Anode Systems

T6:1	Anode type	Adhesion strength without CP (MPa)	Adhesion strength with CP (MPa)	Comments
T6:2	ZRP coating	1.65	2.26	Strength increased after 40 cycles of environmental exposure at 50°C, 90% HR (Reference is present work) Wetting and drying cycles. (Covino et al. 2002)
T6:3	TS zinc coating	1.28–2.29	Up to 3.5	
T6:4	Conductive paint	1.5 (average)	—	Reference is HA specifications, U.K. (Chess and Broomfield 2003)
T6:5	Cementitious overlay	1.5	—	
T6:6	Conductive overlay	3.8	—	Reference Badische Anilin- und Soda-Fabrik (BASF) chemicals

347 cement laitance layer was removed with little or no aggregates
348 exposed, produced better bond strength than that obtained for the
349 VHR profile, in which most of the aggregates were exposed.

350 Various studies carried out in the United States and Canada for
351 the TS zinc/concrete interface to investigate the adhesion mechanism(s), which included the scanning electron microscopy (SEM)
352 and metallographic examinations, confirmed that the adhesion of TS zinc coating on the concrete surface is purely mechanical
353 (Covino et al. 2002). Similar studies with ZRP was outside the scope of the present investigations, but the application of both
354 TS zinc and ZRP coating results in producing a layer of pure zinc on the concrete substrate with the contra distinction that the
355 deposition of a solid zinc layer on a concrete surface and inside concrete is because of solvent evaporation rather than solidification of
356 molten zinc affecting the cold concrete surface, as is the case for TS zinc coating. On the basis of the fact that the ZRP is applied
357 in a liquid form, it is likely that the paint will penetrate the concrete surface and solidified. It is therefore likely that the bond is
358 a chemical/mechanical one, with the physical interlock occurring in the cement pore. Subsequent exploratory examination of the
359 concrete/ZRP interface under SEM (Figs. 6 and 7) showed that the ZRP has definitely penetrated deep into the concrete surface.
360 The total thickness of ZRP, i.e., the light gray area in the photomicrograph, appeared to be approximately 400 μm, but the measured
361 coating thickness on the concrete was between 253 and 282 μm into the concrete matrix, as shown in Fig. 5. This suggested
362 that ZRP penetration into the concrete matrix is approximately 120–150 μm. However, further investigation is required to identify
363 the interfacial chemistry of ZRP.

364 A considerable amount of technical information is available in the literature for the interfacial chemical and electrochemical reactions
365 at the TS zinc coating and concrete. The interfacial chemical and electrochemical reactions at the ZRP coating and concrete are
366 considered to be similar to those identified by the studies carried out in the United States and Canada for the TS zinc/concrete interface
367 (Covino et al. 2002). This is because of one common factor for both TS zinc and ZRP that a solid and pure zinc layer formed on the
368 concrete substrate. When zinc is used as an anode for the CP system, either the galvanic mode or ICCP mode, the reaction steps are
369



373 At the cathode, i.e., rebar, the usual reaction is



375 The preceding anodic reactions lead to the formation of zinc minerals, such as zinc oxide (ZnO)/Zn(OH)₂, followed by secondary
376 mineralization when combined with other constituents of the environment, such as chloride, sulphate, or carbonate ions or
377

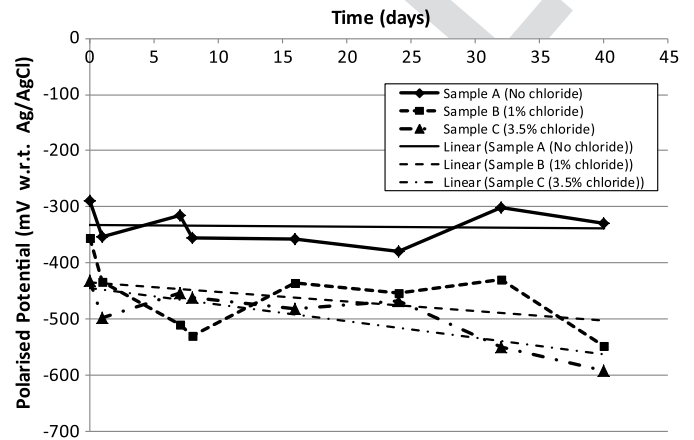


Fig. 6. Polarization and potential shift over 40 cycles of environmental test

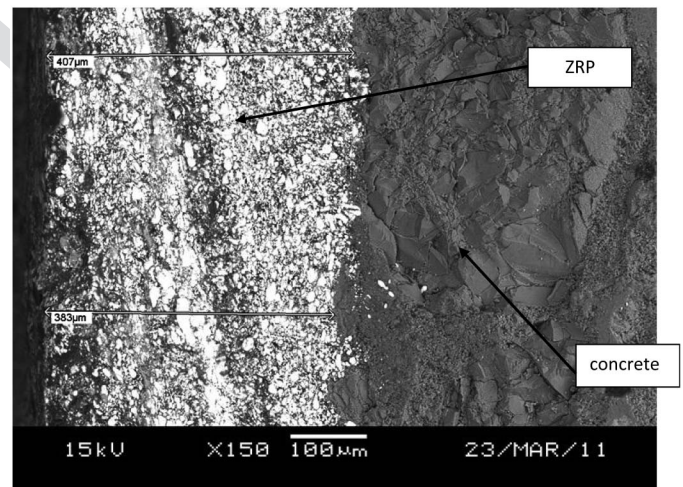


Fig. 7. SEM photomicrograph of ZRP specimen

381 minerals in the cement paste to form complex minerals, such as
382 zinc hydroxycarbonate, zinc hydroxychloride, and zinc hydroxy-
383 sulphate. With the passage of time, the more stable of these min-
384 erals will predominate over the less stable minerals in the Zn oxide
385 layer, which is likely to precipitate at the anode (zinc)-concrete in-
386 terface. The zinc corrosion products, particularly zinc oxychloride
387 and zinc oxysulphate, are formed by electromigration of chloride
388 and sulphate ions from within the concrete to the anode (Covino
389 et al. 2002). Further, as zinc ions migrate into concrete, a reaction
390 zone is developed in the cement paste, with zinc replacing Ca and
391 forming a (Ca, Zn) aluminosilicate. All these may affect the bond
392 strength of the zinc coating, leading to premature failure of the
393

403 anode. However, as discussed in the next section, the results obtained after 40 cycles of accelerated testing in an environmental chamber with an applied CP current density of 440 mA/m², which is four times the current density applied to the anode recommended in the National Association of Corrosion Engineers (NACE) standard and in accordance to BS EN 12696 or 200 times the current density used in the Oregon DOT specification, showed some increase in bond strength (Covino et al. 2002).

411 Environmental Durability

412 The durability, i.e., anode life, and effective performance of the zinc coating, both TS zinc or ZRP, largely depends on adhesion (bond strength) between the anode and concrete, which in turn is affected by various factors, such as environmental exposure conditions, e.g., humidity, temperature, and chloride, concrete surface preparations, and, more importantly, the chemical/electrochemical reactions at the zinc-concrete interface because of application of the CP current. The durability of zinc anodes can be defined in terms of electrochemical aging, as determined from the total electrical charge passed until the adhesion (bond) strength of the zinc coating decreased to zero (Covino et al. 2002).

423 The data collected at the end of the durability testing in the environmental chamber show that the total charge passed in 40 cycles was calculated to 427 A-h/m². In accordance with the NACE standard TM0294 (NACE 2007), the total charge density of

38,500 A-h/m² of the actual anode surface area equates to a serviceable anode life of 40 years if operated at a current density of 110 mA/m² of the anode surface for 40 years (NACE 2007). This represents a predicted anode life of approximately 20 years at a normal operating current density of 10 mA/m² or some 100 years at 2.2 mA/m², as recommended by the Oregon DOT specification (Covino et al. 2002).

434 The results of the environmental testing given in Tables 7 and 8 were recorded at a 20°C temperature and 50% humidity, without and with application of CP. The polarized potentials and CP current of the reinforcements monitored during the 40 cycle environmental testing (Fig. 6) showed increased levels of polarization on all cube samples, and the results also showed that the higher the potential shift, i.e., instant off polarized potential minus base corrosion potential, the higher the chloride content in the concrete. The analysis of the corrosion currents for the cube specimens, calculated from the measurements using macrocell corrosion probes, show that the average corrosion of rebars without CP increased with chloride content from 46 to 57 μA for 0% Cl and 1–3.5% Cl, respectively, as expected. This is in line with the increasing risk of corrosion with increasing levels of chloride in the concrete, as indicated by the measured corrosion potentials. Similarly, with CP, the higher the measured average flow of corrosion currents, rather than the protection current, from the ZRP anode system, the higher the chloride content in the concrete. At the end of 40 cycles, i.e., 40 days, of the durability test, the adhesion strength of the ZRP concrete was

Table 7. Corrosion Potential versus Silver/Silver Chloride Reference Electrode and Corrosion Current of Rebar in Cube Samples Without CP

T7:2	Number of days recorded	Cube A (no chloride content)		Cube B (1% chloride content)		Cube C (3.5% chloride content)	
		Corrosion potential (mV)	Corrosion current (μA)	Corrosion potential (mV)	Corrosion current (μA)	Corrosion potential (mV)	Corrosion current (μA)
T7:3	1	-306	-38	-358	-39.5	-370	-39
T7:4	2	-318	-47	-368	-42	-405	-39.5
T7:5	3	-298	-40	-361	-40	-417	-37
T7:6	4	-279	-49.5	-342	-44	-428	-42
T7:7	5	-271	-47	-357	-48.5	-453	-53.5
T7:8	6	-283	-47.5	-354	-52	-461	-52.5
T7:9	7	-248	-48	-312	-55	-414	-50
T7:10	8	-259	-40	-368	-59	-434	-49.5
T7:11	9	-273	-49	-363	-63	-438	-53.5
T7:12	10	-289	-53	-357	-72	-440	-62
T7:13	11	-292	-48	-344	-68	-412	-67
T7:14	12	-301	-47	-343	-75	-471	-73
T7:15	13	-312	-42	-396	-73.5	-449	-82
T7:16	14	-318	-49	-356	-74	-453	-93

Table 8. Corrosion Potential versus Silver/Silver Chloride Reference Electrode and Corrosion Current of Rebar in Cube Samples with CP

T8:2	T8:1	Number of days	Cube A (no chloride)		Cube B (1% chloride)		Cube C (3.5% chloride)	
			Polarized potential with respect to Ag/AgCl (mV)	Calculated macrocell corrosion current (μA)	Polarized potential with respect to Ag/AgCl (mV)	Calculated macrocell corrosion current (μA)	Polarized potential with respect to Ag/AgCl (mV)	Calculated macrocell corrosion current (μA)
T8:3	1	-353	-49.5	-433	-73.5	-498	-93.5	
T8:4	7	-315	-52	-510	-75	-453	-98	
T8:5	8	-355	-52.5	-529	-74.5	-461	-98	
T8:6	16	-358	-53	-436	-75	-482	-97.5	
T8:7	24	-380	-52.5	-453	-75.5	-467	-98.5	
T8:8	32	-301	-52	-430	-76	-549	-98.5	
T8:9	40	-330	-53.5	-548	-76.5	-591	-98	

Note: The measured base potential for Cubes A–C was -289, -356, and -435 mV, respectively. The calculated potential shift at the end of 40 cycles for Cubes A–C was 41, 192, and 159 mV, respectively.

Table 9. Bond Strength Test Results of All Three Cubes before and after Applied Current (Durability Test)

T9:1	Sample	Test results before current (MPa)	Test results after current (MPa)
T9:2	A	1.50	2.0
T9:3	B	1.85	2.5
T9:4	C	1.60	2.3

453 determined, and the results given in Table 9 indicated a significant
454 increase in bond strength, possibly because of electrochemical
455 aging.

456 Electrochemical Performance: Polarization Tests

457 Tables 10 and 11 summarize the results of the investigation to assess
458 various electrochemical parameters. The results showed that the
459 ZRP anode system was capable of polarizing the steel rebar cathod-
460 ically, and the potential shift, i.e., instant off polarized potential
461 minus base corrosion potential, values were found to be increasing
462 with an increased applied current density on the anode the higher
463 the extent of polarization. As expected, the higher the levels of
464 polarization, the higher the chloride content in the concrete.

465 The cumulative charge in kilocoulombs/m² passed across the
466 anode per unit area during the accelerated ICCP test to assess
467 durability is calculated to be approximately 377 kC/m² (Table 10).
468 This equates to 18.2 μm of Zn dissolved. These data can then be
469 used to estimate the design life of the ZRP anode in terms of Zn
470 anode consumption and/or electrochemical aging.

471 Adhesion tests, i.e., pull-off tests using sellotape, at the end of
472 electrochemical testing showed no decrease in the bond strength
473 but some increase in bond. Table 11 gives the polarized potentials
474 of the concrete beam specimens with 0, 2, and 4% chloride, mea-
475 sured at a distance of 200 mm (Reference Cell #1), 400 mm
476 (Reference Cell #2), and 600 mm (Reference Cell #3) away from
477 the primary anode connections for the applied current density of
478 104 mA/m². Similar sets of data were obtained at an applied cur-
479 rent density of 208 and 313 mA/m². These electrochemical tests
480 also showed that there is very little variation of polarized potential
481 with distance from the primary anode. This suggest that the current
482 throwability from the primary anode connection extends at least up
483 to 600 mm without significant current attenuation and confirmed
484 uniform current distribution. This suggests that the ZRP coating
485 is capable of distributing the protection current uniformly.

486 The data generated from this investigation not only provide use-
487 ful information with regard to the performance and suitability of
488 ZRP coatings as a promising anode for the ICCP system, but
489 the service life of the anode could be predicted in accordance with
490 the NACE standard TM0294 (NACE 2007). The ZRP coating used
491 as an ICCP or galvanic mode anode is a consumable anode,
492 whereas ICCP systems are designed to usually utilize nonconsum-
493 able anodes, such as MMO/Ti. Traditionally, the service life of con-
494 sumable anodes is determined using typical anode parameters and
495 can be expressed as follows:

$$\text{Anode life} = \frac{[\text{Faraday consumption rate (A-h/kg)} / \text{number of hours in a year}] \times \text{anode mass (in kg)} \times \text{anode efficiency} \times \text{utilization factor}}{\text{anode current in amperes}}$$

496 However, this traditional approach to calculate the service life of
497 ZRP coating and also TS zinc coating applied on the concrete sur-
498 face may prove to be inappropriate. The service life for the surface-
499 applied zinc anode would, more importantly, depend on the long-
500 term adhesion (bond) strength, which in turn, among other factors,
501 is strongly affected by the chemical/electrochemical reaction
502 products at the zinc-concrete interface. However, for the design
503 calculations, the service life of ZRP, on the basis of charge in
504 kilo-coulombs/m² passed across the anode per unit area, was found
505 to be well in excess of 20 years at a normal operating current
506 density of 10 mA/m².

507 Conclusions

508 On the basis of the results of this investigation and the interpreta-
509 tion and discussions of the results, the following conclusions
510 are made:

- 511 1. The ZRP coating used had good adhesion properties to a con-
512 crete substrate. The adhesion values obtained were 3.5 and
513 1.65 MPa, with and without applied current, respectively.
514 The bond strength results showed that the strength value in-
515 creased between zinc paint and concrete when the current
516 was applied for 40 days. This increase in bond strength is
517 probably because of the chemical/electrochemical reactions
518 between ZRP and cement.

Table 10. Summary Results for Total Charge Passed: Polarization Beam Specimen with 0% Chloride

T10:1	Beam	Applied current (mA)	Applied current density (mA/m ²)	Elapsed time (days)	Total charge passed (kC/m ²)	Cumulative charge passed (kC/m ²)	Amount of Zn dissolved, kC/m ² × 0.048 (μm)
T10:2	1 (no chloride)	10	104	7	62.9	377.4	18.12
T10:3		20	208	7	125.8		
T10:4		30	313	7	188.5		

Note: Similar results were obtained with other chloride content.

Table 11. Summary Results: Polarization Beam Specimen with 0, 2, and 4% Chloride at 104 mA/m²

T11:2	Specimen	Polarized Potentials with respect to Ag/AgCl after 7 days at applied current density of 104 mA/m ²		
		Reference Cell # 1, 200 mm from primary anode connection	Reference Cell # 2, 400 mm from primary anode connection	Reference Cell # 3, 600 mm from primary anode connection
T11:3	Beam with 0% chloride	-385	-387	-389
T11:4	Beam with 2% chloride	-442	-442	-453
T11:5	Beam with 4% chloride	-501	-501	-453

- 519 2. Accelerated environmental test results showed that the ZRP
520 coating was capable of withstanding/supporting high levels
521 of current. More than 300 mA/m² CP current was applied
522 for a total of 40 cycles without showing any evidence of coat-
523 ing deterioration or loss of bond strength.
- 524 3. In accordance with NACE standard TM0294 and on the
525 basis of data obtained from accelerated environmental testing,
526 the service life of the ZRP coating was estimated to be well in
527 excess of 20 years at an applied current density of 10 mA/m².
528 However, the service life of ZRP or TS zinc coating would,
529 more importantly, depend on the chemical/electrochemical
530 reactions at the zinc coating–concrete interface and the nature
531 and extent of the reaction products, i.e., the primary and sec-
532 ondary mineral deposits because of dissolution of zinc as the
533 CP anode, which in turn affects the adhesion strength of the
534 coating to concrete substrate.
- 535 4. Electrochemical tests also showed that there is very little var-
536 iation of polarized potential with distance from the primary
537 anode. This suggests that the current throwability from the pri-
538 mary anode connection extends at least up to 600 mm without
539 significant current attenuation and uniform current distribution.

540 Acknowledgments

541 The authors wish to express their gratitude and sincere appreciation
542 to the laboratory staff of Coventry University.

543 References

- 544 Abreu, C. M., Espada, L., Izquierdo, M., Merino, P., and Novoa, X. R.
545 (1997). "Zinc rich powder coatings in sea water." *Eurocorr'96*,
546 L. Fedrizzi and P. L. Bonora, eds., Vol. 20, Acropolis, Nice, France, 23.
- 547 Abreu, C. M., Izquierdo, M., Keddani, M., Novoa, X. R., and Takenouti, H.
548 (1996). "Electrochemical behaviour of zinc- rich epoxy paints in 3%
549 NaCl solution." *Electrochim. Acta*, 41(15), 2405–2415.
- 550 Amo, B. D., and Giùdice, C. A. (1990). "Influence of some variables
551 on behaviour of zinc-rich paints based on ethyl silicate and epoxy
552 binders." *Proc., 6th Int. Corrosion Congress*, Associazione Italiana
553 di Metallurgia, Florence, 347.
- 554 Apostolos, J. A. (1984). "Cathodic protection of reinforced concrete by
555 using metallized coatings and conductive paints." *Transportation
556 Research Record 926*, Transportation Research Board, Washington,
557 DC, 222–228.
- 558 Armas, R. A., Gervasi, C. A., Sarli, A. D., Real, S. G., and Vilche, J. R.
559 (1992). "Zinc-rich paints on steel in artificial seawater by electrochemi-
560 cal impedance spectroscopy." *Corrosion*, 48(5), 379–383.
- 561 British Standards Institution. (2000). "Concrete—Part 1: Specification,
562 performance, production and conformity." *BS EN 260-1BSI*, London.
- 563 British Standards Institution. (2012). "Cathodic protection of steel in
564 concrete." *BS EN ISO 12696*, London.
- 565 Bullard, S. J., Cramer, S., Covino, B. (2009). "Final Rep., effectiveness of
566 cathodic protection, SPR 345." National Energy Technology Labora-
567 tory, Albany, OR.

- Chess, P.M., and Broomfield, J. P. (2003). *Cathodic protection of steel in
concrete*, CRC Press. 568
- CIRIA. (1993). "Standard test for repair materials and coatings for
concrete, Part 1: Pull-off tests." *CIRIA technical note 139*, London. 569
- Covino, B. S., Jr., Cramer, S. D., Bullard, S. J., Holcomb, G. R., Russel,
J. H., and Collins, W. K. (2002). "Performance of zinc anodes for
cathodic protection of reinforced concrete bridges." *Final Rep. SPR
364*, Oregon Department of Transportation Research Group, FHWA,
Washington DC. 570
- Das, S. C. (2012). "Zinc rich paint as anode system for cathodic protection
(cp) of reinforced concrete structures and development of corrosion/cp
monitoring probes." Ph.D. thesis, Coventry Univ., Coventry, U.K. 571
- Elcometer. (2004). *Elcometer 106 scale 6: Coatings on concrete adhesion
tester and concrete tensile tester: operating instructions*, Belgium. 572
- Feliu, S., Barajas, R., Bastidas, J. M., and Morcillo, M. (1989). "Mecha-
nism of cathodic protection of zinc-rich paints by electrochemical
impedance spectroscopy." *J. Coating Technol.*, 61(775), 63–69. 573
- Fragata, F. L., Sebrão, M., and Serra, E. T. (1987). "The influence of partic-
le size and metallic zinc content in the behaviour of zinc-rich paints." *J.
Coatings Technol.*, 60(751), 12–16. 574
- Hare, C. H. (1998). "Mechanisms of corrosion protection with surface
treated wollastonite pigments." *J. Protective Coatings*, 14(3), 47–82. 575
- Kepler, J. L., Darin, D., and Lock, C. E. (2000). "Evaluation of corrosion
protection methods for reinforced concrete highway structures." *Struc-
tural engineering and engineering materials SM Rep. No. 58*, Univ. of
Kansas Center for Research, Lawrence, KS. 576
- Lindquist, S. A., Méssaros, L., and Svenson, L. (1985). "Aspects of
galvanic action of zinc-rich paints. Electrochemical investigation of
eight commercial primers." *Oil Colour Chem. Assoc.*, 68, 10. 577
- Morcillo, M., Barajas, R., Feliu, S., and Bastidas, J. M. (1990). "Electro-
chemical behavior of zinc-rich coatings." *J. Mater. Sci.*, 25(5),
2441–2446. 578
- NACE (National Association of Corrosion Engineers). (2007). *NACE
TM0294 test method, accelerated life testing of zinc anode for steel
reinforced concrete*, Houston. 579
- National Cooperative Highway Research Program (NCHRP). (2009).
"Synthesis 398, Cathodic protection for life extension of existing rein-
forced concrete bridge elements." *Report No. 398*, Transportation
Research Board, Washington DC. 580
- Pereira, D., Scantlebury, J. D., Ferreira, M. G. S., and Almeida, M. C.
(1990). "The application of electrochemical measurements to the study
and behaviour of zinc-rich coatings." *Corros. Sci.*, 30(11), 1135–1147. 581
- Sagüés, A. A., and Powers, R. G. (1996). "Sprayed-zinc sacrificial anodes
for reinforced concrete in marine service." *Corrosion*, 52, 508. 582
- Strategic Highways Research Program. (1993). "Cathodic protection of
reinforced concrete bridge elements: A state-of-the-art report." *SHRP-
S-337*, Eltech Research Corporation, National Research Council,
Washington DC. 583
- Vilche, J. R., Bucharsky, E. C., and Giùdice, C. A. (2002). "Application of
EIS and SEM to evaluate the influence of pigment shape and content in
ZRP formulations on the corrosion prevention of naval steel." *Corros.
Sci.*, 44(6), 1287–1309. 584
- Wicks, Z. W., Jr., Jones, F. N., and Pappas, S. P. (1994). *Organic coatings:
Science and technology*, 2nd Ed., Wiley, New York. 585
- Zhang, X. G. (1996). *Corrosion and electrochemistry of zinc*, Plenum,
New York. 586